Conference materials
UDC 532.517.4
DOI: https://doi.org/10.18721/JPM.161.140

Application of machine learning approach for turbulence model improvement for flow around airfoil near stall conditions

A.A. Matyushenko [1]✉, V.D. Golubkov [1], A.V. Garbaruk [1], M.Kh. Strelets [1]

[1] Peter the Great St. Petersburg Polytechnic University, Saint-Petersburg, Russia

✉ alexey.matyushenko@mail.com

Abstract. The work is devoted to the improvement of the k-ω BSL turbulence model for the closure of Reynolds averaged Navier-Stokes (RANS) equations with the use of machine learning (ML) methods. The correction developed for this model enhances its accuracy in calculating airfoil flows at stall angles of attack. Testing of the modified model on the flows around different airfoils reveals its superiority for this type of flows. The results demonstrate efficiency of the ML methods for turbulence model improvement.

Keywords: machine learning, RANS-modeling, stall conditions

Citation: Matyushenko A.A., Golubkov V.D., Garbaruk A.V., Strelets M.Kh., Application of machine learning approach for turbulence model improvement for flow around airfoil near stall conditions. St. Petersburg State Polytechnical University Journal. Physics and Mathematics. 16 (1.1) (2023) 236–242. DOI: https://doi.org/10.18721/JPM.161.140

Материалы конференции
УДК 532.517.4
DOI: https://doi.org/10.18721/JPM.161.140

Использование машинного обучения для улучшения модели турбулентности при обтекании крылового профиля в условиях срыва потока

А.А. Матюшенко [1]✉, В.Д. Голубков [1], А.В. Гарбарук [1], М.Х. Стрелец [1]

[1] Санкт-Петербургский политехнический университет Петра Великого, Санкт-Петербург, Россия

✉ alexey.matyushenko@mail.com

Аннотация. Данная работа посвящена улучшению модели турбулентности k-ω BSL, используемой для замыкания осредненных по Рейнольдсу уравнений Навье-Стокса, при помощи методов машинного обучения. Коррекция, разработанная для этой модели, повышает ее точность при расчете обтеканий крыловых профилей при углах атаки срыва потока. Тестирование модифицированной модели для различных крыловых профилей доказывает приоритетность ее использования для данного типа течений. Результаты демонстрируют эффективность методов машинного обучения для улучшения моделей турбулентности.

Ключевые слова: машинное обучение, RANS-моделирование, срыв потока

Ссылка при цитировании: Матюшенко А.А., Голубков В.Д., Гарбарук А.В., Стрелец М.Х. Использование машинного обучения для улучшения модели турбулентности при обтекании крылового профиля в условиях срыва потока // Научно-технические ведомости СПбГПУ. Физико-математические науки. 2023. Т. 16. № 1.1. С. 236–242. DOI: https://doi.org/10.18721/JPM.161.140

Introduction

Models for closure the Reynolds Averaged Navier-Stokes (RANS) equations have been developed for almost 100 years and up to the present time they occupy a dominant position in solving applied problems of calculating turbulent flows. The main advantages of these models are the simplicity of their implementation and efficiency, as well as the availability of well-established computing technologies for performing calculations using them. This opens up the possibility of carrying out serial calculations necessary for the creation and optimization of new designs. However, even the best RANS models are not universal; provide a reliable prediction of averaged characteristics only for a limited range of relatively simple flows, which serves as a stimulus for numerous studies devoted to the construction of new and improving the accuracy of existing models.

Until recently, the model improvement study was carried out “by hand” and largely relied on physical intuition, and its success largely depended on the experience of researchers, which led to a certain “stagnation” in this area. On the other hand, advances in the development of measurement methods and computing systems have led to the fact that in recent years the knowledge base on the results of physical and numerical experiments with a high accuracy (“reference” data) has significantly expanded and effective tools have appeared that allow analysing large volumes of such data. In this regard, the possibility of improving existing turbulence models based on information obtained from the analysis of “reference” data has opened up. One of the most effective methods for solving this problem are Machine Learning (ML) methods, which allow to analyse and generalize huge arrays of reference data and connect many objects of the training sample with many answers using a special function called the Neural Networks (NN). This function, which is a correction to the model under consideration, can later be used to solve problems that were not included in the training set.

The first works aimed at improving RANS models using “reference” data and machine learning methods were devoted to eliminating the so-called parametric uncertainties caused by inaccuracies in determining the empirical constants of RANS models [1-3]. However, as shown in [4], a much more significant contribution to the discrepancy between the simulation result and “reference” data is made by the so-called structural uncertainties due to the imperfect formulation of the models. This gave impetus to the development of methods aimed at eliminating structural uncertainties by introducing appropriate functional corrections into the model equations [5-7]. However, when using ML methods that use “reference” data to eliminate structural uncertainties, the difficult task of matching between the learning environment (for example, DNS data) and the learning object (RANS model) arises. Thus, according to [8,9], if even very accurate DNS data are used as input data for ML, then the results of RANS modeling supplemented with such ML, contrary to expectations, may turn out to be unsatisfactory.

To eliminate this shortcoming, Duraisamy et al. [10] proposed a two-stage technique for supplementing RANS models with “reference” FIML (Field Inversion and Machine Learning) data. Within the framework of this technique, the result of solving the inverse problem is used as input data for ML, which is the spatial distribution of the correction introduced into the model to eliminate structural uncertainties. Later, this approach was developed and tested by the Duraisamy group on various problems, including the flow around airfoils at high angles of attack [11, 12].

One of the task where computation accuracy can be significantly improved by modification of the turbulence model is flow around airfoils at stall angle of attack where the flow is separated and maximal lift coefficient is achieved. This task is very important for aviation and wind power, as well as for turbomachinery flows. Even the best turbulence models systematically overpredict the maximum lift coefficient and corresponding angle of attack [13].

Recently FIML method was implemented into ANSYS Fluent code. In the current work it is used for improvement of the k-ω BSL [14] turbulence model for the flows around airfoils with the double precision version of ANSYS Fluent 2022R1. The pressure-based coupled solver was employed with the Second Order Upwind discretization scheme for the convective terms in all transport equations. All the presented results are grid and iterative converged.

Considered testcases

Four aerodynamic airfoils were considered for development of the model modification and its verification. S805 airfoil at $\alpha = 11°$ was chosen for the model development, whereas prediction of flow around S805, S809, S827, DU-96-W-180 airfoils in wide range of angles of attack was used during its verification study. Experimental investigations of the considered airfoils [15–18] were carried out in low turbulence wind tunnels (I <1%). at relatively high Reynolds number (Re > 106) based on airfoils chord and freestream velocity. Since the experimental Mach number did not exceed 0.15, incompressible flow is considered. For all cases, the computational domain shown a rectangular shape representing a 2D slice of a wind tunnel test section with the height H corresponding to experimental one. The angle of attack corresponds to the geometrical rotation airfoil in the tunnel. The size of the computational domain and flow parameters are presented in Table 1.

Table 1

Setup parameters for the flow around considered airfoils

Airfoil	H/C	Re	Tu, (%)
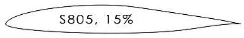	3.6	1×10^6	0.05
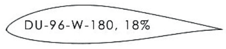	3.0	2×10^6	0.04
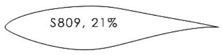	5.0	4×10^6	0.06
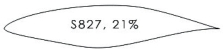	3.0	3×10^6	0.08

Inlet and outlet boundaries are located at a distance of about 10C upstream and downstream of the airfoil leading edge. The boundary conditions are set as follows. Non-slip conditions are specified on the airfoil. A constant velocity is specified at the inlet section of the computational domain. Inlet turbulent kinetic energy corresponds to experimental turbulence intensity and the specific dissipation rate is specified as $\omega = 10 \cdot U_\infty / C$ [14]. No-slip conditions are used on the airfoil surface and constant pressure is specified on the outlet. The computational meshes were refined normal to the wall in order to resolve the viscous sublayer ($\Delta y_1^+ < 1$), near the leading edge in the streamwise direction for a proper resolution of thin boundary layer, and near the trailing edge. This results in about 400 points along the airfoil and a total mesh size of about 100,000 cells.

Modification of the model

The modification was developed by adding source term S_ω in ω equation of the original BSL model:

$$\underbrace{\frac{\partial(\rho\omega)}{\partial t} + \frac{\partial(\rho u_j \omega)}{\partial x_j} = \frac{\gamma}{\nu_t} P_k - \beta\rho\omega^2 + \frac{\partial}{\partial x_j}[(\mu_t + \sigma_\omega \mu_t)\frac{\partial\omega}{\partial x_j}] + 2(1-F_1)\frac{\rho\sigma_{\omega 2}}{\omega}\frac{\partial k}{\partial x_j}\frac{\partial \omega}{\partial x_j}}_{\omega\text{-equation of the original BSL model [14]}} + \mathbf{S}_\omega \tag{1}$$

with

$$\mathbf{S}_\omega = C_\omega \rho \omega^2 \tag{2}$$

where C_ω is a function of non-dimensional parameters, obtained using machine learning methods in several stages. At the first stage the optimized field of C_ω was obtained using the adjoint solver in combination with simple iterative optimizer by minimization of the cost function E

$$C_\omega = C^i_{\omega,adjoint} = C^{i-1}_{\omega,adjoint} - \lambda \frac{\partial E}{\partial C^{i-1}_{\omega,adjoint}}. \tag{3}$$

Here λ is the non-dimensional adaptive parameter responsible for the speed of optimization. The definition of E will be given later.

The second stage is an approximation of the adjoint optimized C_ω field from the first stage by neural network as a function of input non-dimensional parameters:

$$C_\omega = C_{\omega,NN} = NN(input_1,...input_n) \tag{4}$$

Finally the C_ω coefficient was applied to the ω equation and verification study of the modified model (BSL-NN) was performed.

Optimisation of *C*ω field and NN training

As mentioned above, the model modification was developed based on the prediction of flow around S805 airfoil at near stall angle of attack α = 11. For such flow regime the original BSL model delays separation on the suction side and, as consequence, ovepredicts experimental lift coefficient. Therefore the cost function E from Eq. (3) is built based on the difference between the computational C_L and experimental $C_{L\exp}$ = 1.19623 value of lift coefficient (first term) and minimization of C_ω (second term), reads as:

$$E = \left|C_L - C_{L\ \exp}\right| + \beta\sum_{cells}\left(C_{\omega,adjoint}\right)^2. \tag{5}$$

During the adjoint optimization design iterations the computational lift coefficient is adjusted to the experimental value by modification of the C_ω fields shown in Fig. 1 (right). It is well seen that the C_ω is positive on the suction side of the airfoil. Thus $\boldsymbol{S}_\omega$ source term provides the additional dissipation and, as consequence, accelerated separation on the suction side. These effect is confirmed by streamwise velocity contours and streamlines which visualize the separation zone on the suction side of the airfoil for the original and the modified models (Fig. 2). The modification strongly shifts the separation point toward leading edge and increases the size of recirculation zone. This improves the agreement of the computed pressure coefficient with the experimental data (Fig. 3).

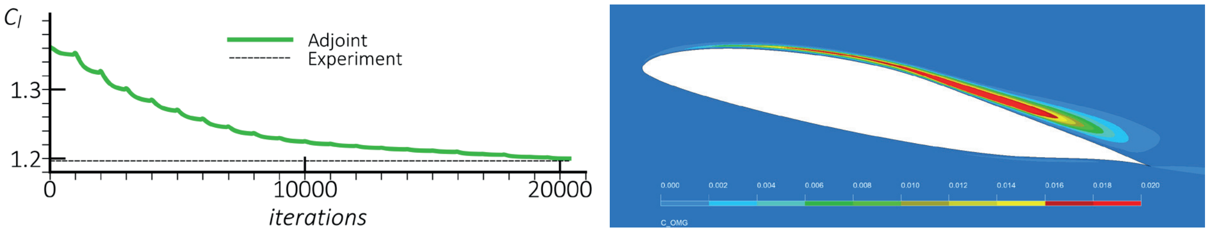

Fig. 1. Convergence history of simple optimizer and optimized C_ω field for S805 airfoil at α = 11°

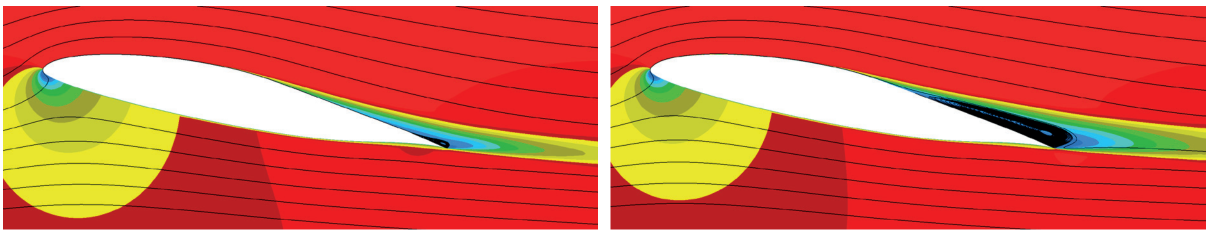

Fig. 2. Contours of streamwise velocity component and streamlines for original (left) and optimized (right) BSL model for S805 airfoil at α = 11°

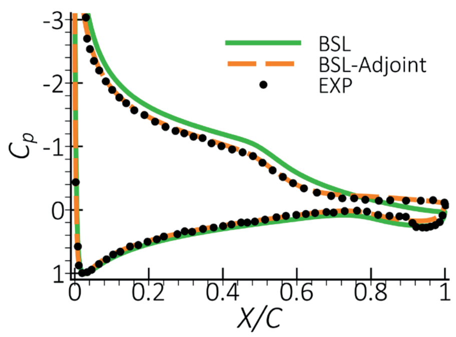

Fig. 3. Distribution of pressure coefficient on the S805 airfoil at α = 11° for the original and adjoint modified BSL model

During NN training of the C_ω is considered as a function of three parameters

$$C_{\omega\,NN} = NN\left(\frac{S}{0.3\omega}, \frac{\sqrt{k}}{0.09\omega d_w}, \frac{\nu_t}{\nu}\right). \tag{6}$$

The training is carried out using three hidden layers (24,16 and 8 nodes) with following activation function:

$$f(x) = \frac{1}{1+|x|}. \tag{7}$$

The comparison of the skin friction and pressure coefficient on the airfoil shown in Fig. 4 demonstrates that the NN results is almost the same as results obtained with the adjoint solver. Taking into account the good agreement of the adjoint results with the experimental data one can see that the modified model also predicts experimental distribution well.

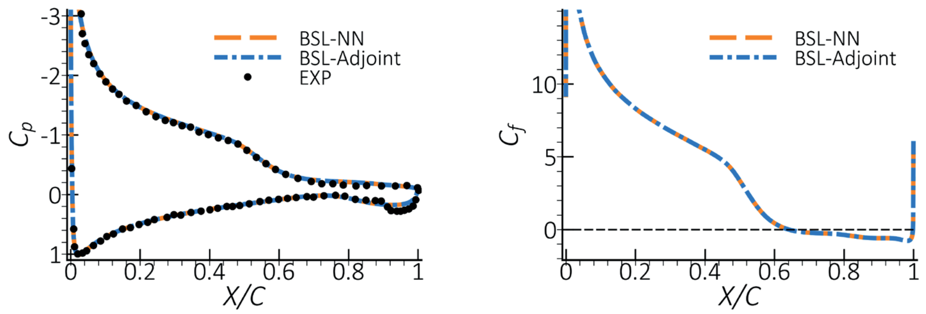

Fig. 4. Distribution of pressure (left) and skin friction (right) coefficient for S805 airfoil at α = 11° predicted with the adjoint and NN modified BSL model

Verification of modified model

Computations using the original and modified versions of the BSL model for the considered airfoils show that both models predict virtually the same lift coefficient for low and angles of attack ($\alpha < 10°$) when the flow is attached (Fig. 5). At higher angles of attack the modified BSL-NN model predicts lower value of the lift coefficient due to the larger size of the recirculation zone. Thus lift coefficient distribution for modified version is in better agreement with the experimental data for all the considered airfoils over a wide range of angles of attack than the original BSL model, which strongly overpredicts lift value. For S827 airfoil BSL-NN model improves prediction of the lift coefficient even at low angles attack due to earlier stall than for other cases. For this airfoil separation on the suction side starts at $\alpha = 1°$. However for some angles of attack in stall regime the BSL-NN results still differ from the experimental data. This phenomenon can be described by the effect of the 3D so-called “mushroom cells” structures in the experiment, which cannot be predicted in 2D setup.

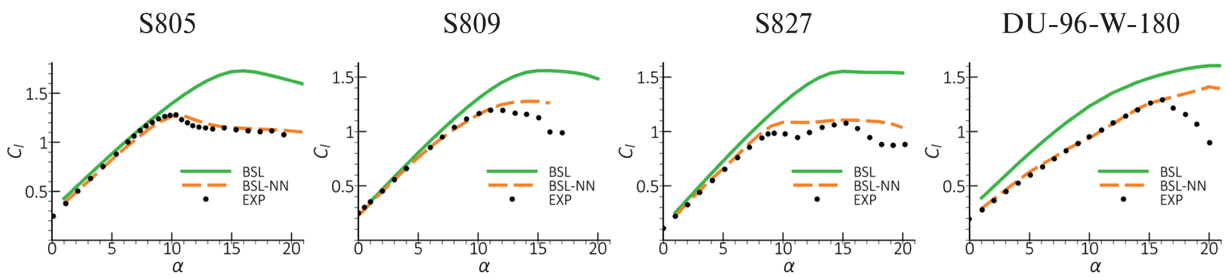

Fig. 5. Comparison of experimental and computational lift coefficient at different angles of attack for original BSL and modified BSL-NN model

Conclusions

Proposed modification of the k-ω BSL turbulence model with machine learning methods significantly improves the accuracy of prediction of aerodynamic characteristics over airfoils in wide range of angles of attack ($\alpha = 0° - 20°$). The results demonstrate the efficiency of the machine learning methods for turbulence model improvement.

Acknowledgements

The results of the work were obtained using computational resources of Peter the Great Saint-Petersburg Polytechnic University Supercomputing Center (http://www.spbstu.ru).

The study was carried out within the framework of the scientific program of the National Center for Physics and Mathematics (project "Mathematical modeling on supercomputers with exa- and zettaflops performance").

REFERENCES

1. **Cheung S.H., Oliver T.A., Prudencio E.E., Prudhomme S. and Moser R.D.,** Bayesian uncertainty analysis with applications to turbulence modeling Reliab. Eng. Syst. Saf. 96 (2011) (9) 1137–1149.

2. **Margheri L., Meldi M., Salvetti M. and Sagaut P.,** Epistemic uncertainties in RANS model free coefficients Comput. Fluids 102 (2014) 315–335.

3. **Edeling W.N., Schmelzer M., Cinnella P. and Dwight R.P.,** Bayesian predictions of Reynolds-averaged Navier–Stokes uncertainties using maximum a posteriori estimates, AIAA J. 5 (6) (2018) 2018–2029.

4. **Papadimitriou D.I. and Papadimitriou C.,** Bayesian uncertainty quantification of turbulence models based on high-order adjoint Comput. Fluids 120 (2015) 82–97.

5. **Dow E. and Wang Q.,** Quantification of structural uncertainties in the k–ω turbulence model, 52nd AIAA/ASME/ASCE/AHS/ASC Structures, Structural Dynamics and Materials Conference, Denver Colorado AIAA April Paper (2011) 2011–1762.

6. **Singh A.P and Duraisamy K.,** Using field inversion to quantify functional errors in turbulence closures Phys. Fluids 28 (2016) 045110.

7. **Xiao H., Wu J.L., Wang J.X., Sun R. and Roy C.,** Quantifying and reducing model-form uncertainties in Reynolds-averaged Navier–Stokes simulations: a data-driven, physics-informed Bayesian approach J. Comput. Phys. 324 (2016) 115–136.

8. **Poroseva S.V., Colmenares F.J.D., Murman S.M.,** On the accuracy of RANS simulations with DNS data Phys. Fluids 28 (2016) (11)

9. **Thompson R.L., Sampaio L.E.B., de Bragança Alves F.A., Thais L. and Mompean G.,** A methodology to evaluate statistical errors in DNS data of plane channel flows Comput. Fluids 130(2016) 1–7.

10. **Duraisamy K., Zhang Z.J., Singh A.P.,** New Approaches in Turbulence and Transition Modeling Using Data-driven Tehniques 53rd AIAA Aerospace Sciences Meeting AIAA SciTech AIAA Paper (2015) 2015–1284.

11. **Parish E.J., Duraisamy K.,** A paradigm for data-driven predictive modeling using field inversion and machine learning J. Comput. Phys. 305 758–774.

12. **Singh A., Medida S., Duraisamy K.,** Machine-Learning-Augmented Predictive Modeling of Turbulent Separated Flows over Airfoils AIAA J. 55 (7) (2017) 2215–2227.

13. **Matyushenko A.A., Kotov E.V. and Garbaruk A.V.,** Calculations of flow around airfoils using two-dimensional RANS: an analysis of the reduction in accuracy St. Petersburg Polytechnical University Journal: Physics and Mathematics 3 (1) (2017) 15–21.

14. **Menter F.R.,** Zonal Two Equation k-ω Turbulence Models for Aerodynamic Flows AIAA Paper (1993) 93–2906.

15. **Somers D.M.,** Design and Experimental Results for the S805 Airfoil NREL/SR-(1997) 440–6917.

16. **Somers D.M.,** Design and Experimental Results for the S827 Airfoil Period of Performance (2005) 1998–1999.

17. **Somers D.M.,** Design and Experimental Results for the S809 Airfoil, NRELSR-(1997)440–6918.

18. **Timmer W.A. and R.P.J.O.M. van Rooij,** Summary of the Delft University Wind Turbine Dedicated Airfoils AIAA Paper (2003) 0352.

THE AUTHORS

MATYUSHENKO Aleksey A.
alexey.matyushenko@gmail.com

GOLUBKOV Valentin D.
golubkovvd@gmail.com
ORCID: 0000-0001-9473-7430

GARBARUK Andrey V.
agarbaruk@mail.ru
ORCID: 0000-0002-2775-9864

STRELETS Michael Kh.
strelets@mail.rcom.ru

Received 17.10.2022. Approved after reviewing 06.12.2022. Accepted 07.12.2022.